Journal of Magnetic Resonance 212 (2011) 174–185

Contents lists available at ScienceDirect

Journal of Magnetic Resonance

journal homepage: www.elsevier.com/locate/jmr

A conformational study of *N*-acetyl glucosamine derivatives utilizing residual dipolar couplings

Markus Kramer, Erich Kleinpeter *

University of Potsdam, Department of Chemistry, Karl-Liebknecht-Str. 24-25, 14476 Potsdam/Golm, Germany

ARTICLE INFO

Article history:
Received 18 April 2011
Revised 22 June 2011
Available online 2 July 2011

Keywords:
NMR
Residual dipolar couplings
Molecular dynamics
N-acetyl glucosamine derivatives
Carbohydrates

ABSTRACT

The conformational analyses of six non-rigid *N*-acetyl glucosamine (NAG) derivatives employing residual dipolar couplings (RDCs) and NOEs together with molecular dynamics (MD) simulations are presented. Due to internal dynamics we had to consider different conformer ratios existing in solution. The good quality of the correlation between theoretically and experimentally obtained RDCs show the correctness of the calculated conformers even if the ratios derived from the MD simulations do not exactly meet the experimental data. If possible, the results were compared to former published data and commented.

1. Introduction

In 2009 Fettke et al. reported about the syntheses and conformational studies of *N*-acetyl glucosamine (NAG) derivatives [1]. Thio-saccharides derived from NAG are of interest as potential chitinase inhibitors and thus as possible insecticides, fungicides, antimalaria or antiasthmatics. To understand this inhibition a conformational study of suitable saccharides in a physiological medium in free and protein-bound state is of great interest. Here we present the structural behaviour of six saccharides given in Table 1, which have been synthesized in the same manner as presented before [1,2].

Fettke et al. performed the conformational analyses of similar compounds employing theoretical grid-searches and experimental NMR methods such as NOESY and the evaluation of scalar coupling constants [1]. Because all investigated molecules (Table 1) are not rigid, this traditional approach leads only to a limited number of constraints, which are additionally difficult to interpret [3].

During the last years residual dipolar couplings (RDC) in combination with computational methods have proved to be a powerful tool for the conformational analysis of both rigid and flexible organic molecules especially carbohydrates in solution [3–9].

The direct dipolar coupling between two spin-½ nuclei *I* and *S* is given by the following equation [10],

$$D_{IS} = -\left(\frac{\mu_0}{4\pi}\right)\frac{\gamma_I\gamma_S h}{2\pi^2\langle r_{IS}^3\rangle}\left\langle\frac{3\cos^2\theta-1}{2}\right\rangle \quad (1)$$

with the magnetic constant μ_0, the gyromagnetic ratios γ_I and γ_S of spin *I* and *S*, Planck's constant *h*, the distance r_{IS} between *I* and *S*, and the angle θ between the static magnetic field B_0 and the internuclear vector. The brackets indicate a time average over all existing molecular motions i.e. tumbling and internal dynamics. In the isotropic case $\langle 3\cos^2\theta - 1\rangle$ averages to zero and D_{IS} also reaches this value, whereas in the anisotropic aligned case D_{IS} becomes measurable. This molecular alignment has to be weak, which means that only about 0.05% of the solute molecules are oriented at the same time, otherwise the resolution of the NMR spectra will be too low for an evaluation. This can be achieved by several media [11]. In our case we chose the 1,2-dimyristoyl-*sn*-glycero-3-phosphocholine (DMPC)/1,2-dihexanoyl-*sn*-glycero-3-phosphocholine (DHPC) and pentaethylene glycol monododecyl ether ($C_{12}E_5$)/*n*-hexanol systems, which were successfully used to orient carbohydrates [5,7,12] and biomolecules in general [13].

2. Results and discussion

Different standard NMR experiments (^{1}H, ^{13}C, COSY, HSQC, HMBC, NOESY, TOCSY (only for **6**)) were performed in order to assign all NMR signals (Fig. 1).

The anomeric configuration of each substance was determined by evaluating the $^3J_{H_1,H_2}$ coupling constants. Table 2 shows the $^3J_{H_1,H_2}$ values derived from the signal of the H-1 proton at the given position.

The lower electronegativity of sulfur in the S-linked aglycones results in a higher vicinal coupling constant compared to the values for the substances containing an oxygen linkage [2,14,15]. All

* Corresponding author. Fax: +49 331 977 5064.
E-mail address: ekleinp@uni-potsdam.de (E. Kleinpeter).

1090-7807/$ - see front matter © 2011 Elsevier Inc. All rights reserved.
doi:10.1016/j.jmr.2011.06.029

Table 1
Investigated carbohydrates.

Substance	Structure
1	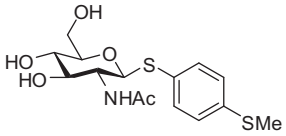
2	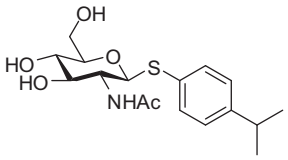
3	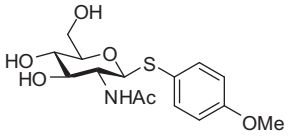
4	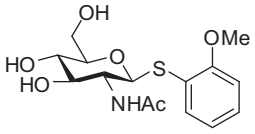
5	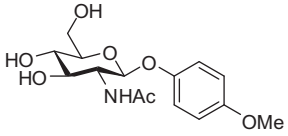
6	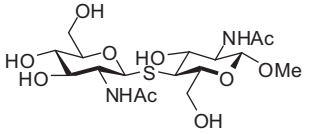

measured couplings lie in between the Karplus-range of a torsional angle of 180°, which corresponds to a β-configured anomeric carbon atom for all substances.

The one-bond ^{13}C–^{1}H RDC ($^{1}D_{C,H}$) values were extracted from F_2-coupled HSQC experiments (CLIP-HSQC, [16]) and are shown in Table 3; the denomination of atoms is given in Fig. 2. The maximum errors of the RDC values are propagated from the individual maximum errors of the $^{1}J_{C,H}$ and $^{1}J_{C,H} + {}^{1}D_{C,H}$ couplings which were determined by the signal shift method explained in [17]. Substance **6** was measured in two different alignment media (DMPC/DHPC bicells and $C_{12}E_5$/*n*-hexanol) because we wanted to know which influence the used medium has on the conformer ratio. For the other substances this was unfortunately not possible, because its solubility in the $C_{12}E_5$/*n*-hexanol system was too low to get suitable HSQC spectra.

The conformations of the investigated (pseudo-)disaccharides are principally defined by the torsional angles Φ and Ψ formed between the NAG unit and the glycosidic residue (Fig. 3).

To figure out the possible values for Φ and Ψ MD simulations have been performed using the TINKER software package [18] and considering the influence of water as solvent employing the periodic boundary condition (PBC). The analysis of the results, was carried out with the aid of the program VMD [19] for plotting the respective torsional angle against the simulation time (see Supplementary material) and to get Φ/Ψ-plots for each carbohydrate (Fig. 4).

As shown in the Φ/Ψ-plots for substance **1**–**4** four and for **5** and **6** two combinations of Φ and Ψ are possible, whereas the Φ and Ψ angles of all conformers lie in between a range of about ±30°. For **5** the exchange of sulfur with oxygen leads to a shorter C–O bond length of 1.42 Å (1.83 Å for C–S), which produces stronger steric interactions between the aglycone and the hexose unit and consequently causes only two conformers. These values are in agreement with that reported previously [1].

Because the aglycones of **1**–**3** and **5** are symmetric, the number of combinations reduces to two for **1**–**3** and one for **5**, respectively. This finally leads to one conformation for **5**, two conformations for **1**–**3** and **6** and four conformations for **4** that have to be considered. In a next step the population of each conformation has to be defined by counting the number of points of any region in the Φ/Ψ-plots (Table 4). A total of 40,000 dumps were obtained from the MD simulations.

For each region one representative conformer was extracted from the MD simulated frame with the lowest total potential energy. The dihedral angles of the resulting conformers are shown in Table 5.

For the subsequent calculation of RDC values, we assumed that the alignment of the conformers of each substance can be described by a single alignment tensor. This seem to be appropriate because the overall shape of the conformers in the ensembles is similar (Table 6) [20]. To simulate the orientation of the calculated conformers per substance in the alignment medium, we performed an RMSD fit of the atomic coordinates of the entire molecule, excluding the flexible hydroxyl protons [21].

The atomic positions and conformer ratios thus obtained were now used in the calculations of the theoretical $^{1}D_{C,H}$ values, which were performed with REDCAT [22] using the "AVG" keyword as explained in the tutorial [21,23]. As a criterion for the quality of the calculated values, the number of solutions, the RMSD between theoretical and measured RDCs and the quality-factor (*Q*-factor; Eq. (2)) were used.

$$Q = \sqrt{\left(\frac{\sum_{i=1}^{N} (D_i^{exp} - D_i^{calc})^2}{\sum_{i=1}^{N} (D_i^{exp})^2} \right)} \tag{2}$$

where D_i^{exp} is the measured RDC; D_i^{calc} the calculated RDC; N the total number of RDCs; and i is an index running from 1 to N.

For each substance different fractions of the corresponding conformers were taken into account aiming at gaining that ratio delivering a maximum number of solutions and a minimum RMSD and *Q*-factor. We started every calculation with that conformer ratio obtained from the MD simulations and successively increased the percentage of the favored conformer to check if the correlation between calculated and experimental $^{1}D_{C,H}$ could be improved (Table 7). To confirm the correctness of the ratios thus obtained, a recalculation was executed taking only the non-populated conformers into account. The marked $^{1}D_{C,H}$ values in Table 3 had to be omitted during the calculations because due to peak broadening or signal overlapping it was not possible to determine them correctly.

In DMPC/DHPC bicells the best correlation for substance **1**–**4** and **6** was achieved if only the favored conformer was considered, while for **5** it could be proved that the solely calculated conformer is also the only existing conformer in solution (Table 8). The similar results for conformer A and B of substance **4** can be traced back to the fact that conformer A is obtainable from conformer B by rotating the dihedral angle Ψ by approximately 180°. As shown in Eq. (1) the RDC values depend on the orientation of the spins along the static magnetic field (θ), which is contained in the expression $\langle 3\cos^2\theta - 1 \rangle$. Because the value of $\cos^2\theta$ does not change if θ is changed by 180°, the whole expression will not change and thus the RDC values for both conformers are equal or, as in our case, at least similar. The better results for conformer B and the observed

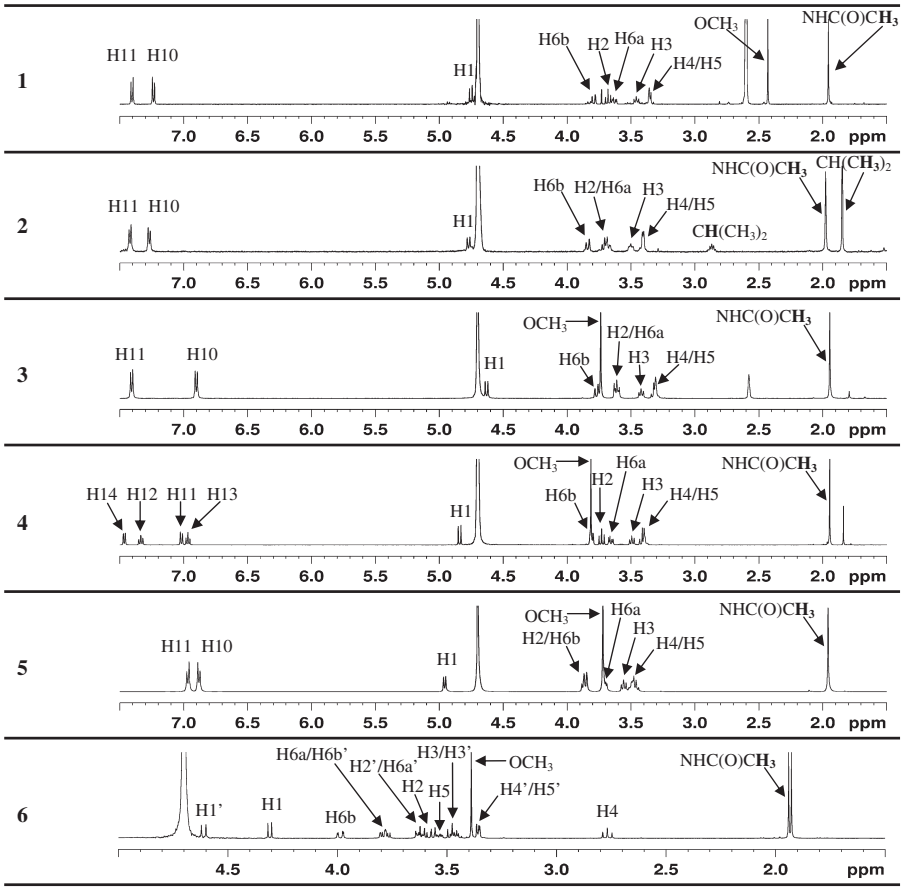

Fig. 1. ^{1}H NMR spectra of **1**–**6** with signal assignment (the signals were marked with the corresponding denomination of the atoms from Fig. 2; all spectra were referenced to the HDO signal at 4.7 ppm).

Table 2
$^{3}J_{H_1,H_2}$ coupling constants to determine the configuration of C1.

Substance	δ (ppm)	$^{3}J_{H_1,H_2}$ (Hz)	Solvent
1	4.76	10.48	D_2O
2	4.77	10.29	D_2O
3	4.65	10.36	D_2O
4	4.84	10.42	D_2O
5	4.96	8.48	D_2O
6	4.33	8.51	D_2O
	4.63	10.46[a]	D_2O

[a] $^{3}J_{H_{1'},H_{2'}}$.

NOEs finally proved, that conformer A is too low populated to get the NOEs and thus can be disregarded.

In $C_{12}E_5$/*n*-hexanol a conformer ratio of 1:16 and 0:1 (**6**A:**6**B) for substance **6** led to almost equal results.

The results for the substances **1**–**5** correlate well with the NOEs that could be observed (Fig. 5). In the aromatic region of the NOESY spectra for **1**–**3** and **5** there is only one strong NOE between H10/H10′ and H1 and for **4** between H14 and H1 observable (Fig. 6; for the complete spectra see Supplementary material). For **1**–**3** the NOE H10/H10′–H2 and for **4** the NOEs OMe–H1, OMe–H2 and H14–H2 which should be observable in presence of the remaining conformers are missing.

The calculated conformers for substance **6** should also be distinguishable via different NOEs produced by the protons H1′–H3 and H1′–H4, respectively. Among all observed NOEs for proton H1′, the only interglycosidic NOE which seems to be present is that observed between H1′ and H4. The protons H3′ and H3 have a similar chemical shift, so it is difficult to decide whether H3 contributes to the NOE H1′–H3′. Zooming in on that peak it becomes obvious that there is a small contribution of H3 (Fig. 7), which means a discrepancy in the observed conformers derived from the NOESY experiment and the RDC measurements in bicelle media. The RDCs from the measurements in $C_{12}E_5$/*n*-hexanol are in good agreement with a conformer ratio of 0:1 and 1:16 (**6**A:**6**B) for substance **6**. The observed NOE H1′–H3 gives rise to the conclusion that conformer **6**B has a population higher than 1%, which disagrees with the ratio 0:1. These two results for substance **6** depending upon the alignment medium can be attributed to the different strength each conformer is aligned in it. In DMPC/DHPC bicells only the conformer **6**B will align resulting in RDC values, reflecting only this conformation, which disagrees with the measured NOEs. In $C_{12}E_5$/*n*-hexanol both conformers **6**A and **6**B are aligned, but with a ratio different to that observed in the MD simulations.

To compare these results with that published earlier by Fettke et al. [1], we had to determine a second set of dihedral angles formed by the atoms H1′–C1′–S–C4 for Φ and C1′–S–C4–H4 for Ψ, because the atoms used to describe the torsional angles in [1] are not consistent with the IUPAC nomenclature we used. This finally leads to the values shown in Table 9.

In [1] our calculated conformations possess the highest relative energy and hence should be less populated, while the other two conformations reported could not be confirmed. This can be

Table 3
Measured $^1D_{C,H}$ values with maximum errors.

RDC	*Substance*	**1**	**2**	**3**	**4**	**5**	**6**	
	Medium	Bicells	Bicells	Bicells	Bicells	Bicells	Bicells	$C_{12}E_5$/*n*-Hexanol
C1–H1		−1.2 ± 0.4	1.5 ± 0.6	−1.1 ± 1.1	−4.9 ± 0.9	0.5 ± 1.1	9.6 ± 0.9	5.4 ± 1.5
C2–H2		−1.5 ± 0.9	−4.2 ± 1.1	0.0 ± 1.1	−7.6 ± 3.4[a]	−1.3 ± 1.3	7.9 ± 0.7	6.6 ± 3.1[a]
C3–H3		−1.4 ± 1.0	−2.7 ± 1.1	−3.5 ± 0.6	−9.7 ± 0.9	−1.8 ± 1.0	10.9 ± 5.0[a]	5.6 ± 1.5
C4–H4		0.3 ± 0.7	−0.9 ± 0.3	2.3 ± 0.7	−4.2 ± 1.1	−2.5 ± 0.9	10.7 ± 1.0	6.2 ± 1.7
C5–H5		0.9 ± 0.9	2.5 ± 1.0	−1.4 ± 0.8	−6.2 ± 0.9	−2.6 ± 1.1	9.4 ± 0.6	4.0 ± 1.9
C10–H10		−2.3 ± 0.9	−1.8 ± 1.0	1.7 ± 1.1	–	0.1 ± 0.8	–	–
C11–H11		−3.2 ± 1.0	7.8 ± 0.9	0.6 ± 1.1	−1.9 ± 0.8	−1.0 ± 0.9	–	–
C12–H12		–	–	–	10.4 ± 0.9	–	–	–
C13–H13		–	–	–	−11.9 ± 0.9	–	–	–
C14–H14		–	–	–	−2.6 ± 0.7	–	–	–
C1′–H1′		–	–	–	–	–	6.2 ± 0.6	6.6 ± 1.0
C2′–H2′		–	–	–	–	–	8.2 ± 1.2	10.1 ± 1.4
C3′–H3′		–	–	–	–	–	10.2 ± 0.6	1.4 ± 1.5
C4′–H4′		–	–	–	–	–	3.2 ± 0.9	2.6 ± 1.8
C5′–H5′		–	–	–	–	–	5.6 ± 1.0	6.0 ± 1.3

The average error in the measurements depends on the alignment medium and is ±1.0 Hz for DMPC/DHPC bicells and ±2.0 Hz for $C_{12}E_5$/*n*-hexanol.
[a] Values were omitted during calculations.

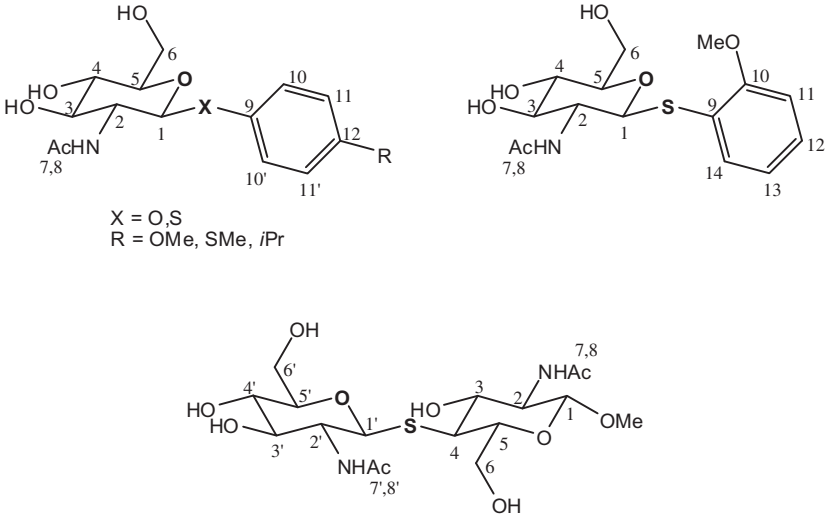

Fig. 2. Denomination of the atoms in the investigated carbohydrates.

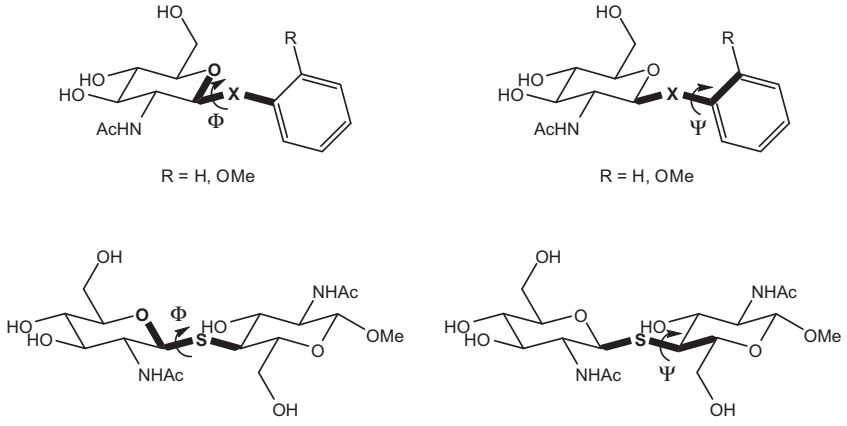

Fig. 3. Graphical representation of the torsional angles Φ and Ψ.

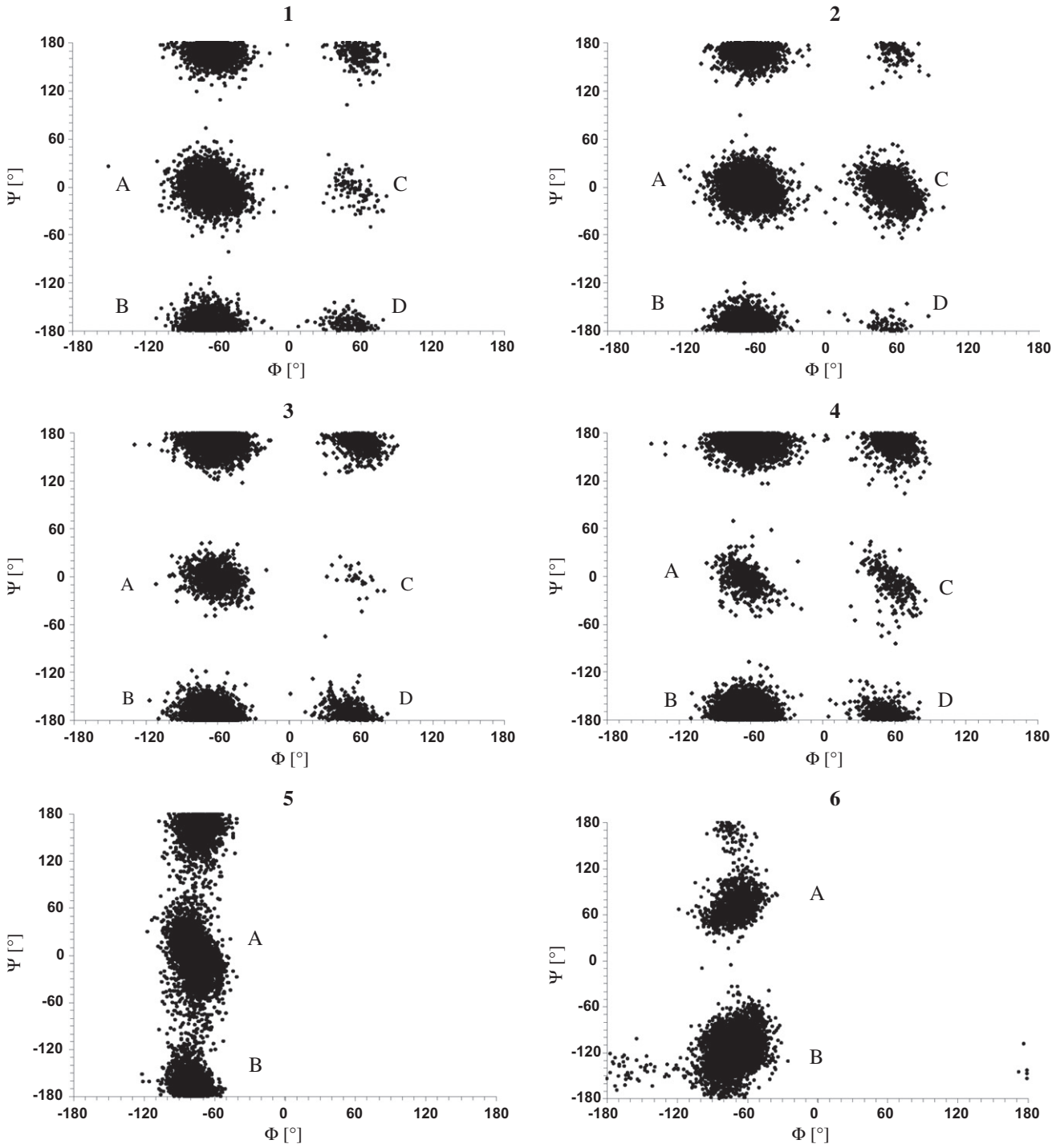

Fig. 4. Φ/Ψ-plots from the MD simulations.

explained by the different computational methods used to calculate the possible conformers of **6**.

Furthermore, the substances **1** and **5** are parts of the investigated oligosaccharides **3** and **5** in [1], so that it is indicated to compare the corresponding torsional angles. The left non-reducing part of these oligosaccharides should not have a strong steric influence on the conformation of the aromatic aglycone and can therefore be treated separately to a certain degree. A comparison needs again a redetermination of the appropriate angles, resulting in the values shown in Table 10.

The deviation of Φ for conformer A of substance **1** from Φ for conformer F of substance **3** in [1] is indeed large, but lies in between the calculated range of ±30° for this dihedral angle. The other calculated conformers **3**G/G′ and **5**F/F′ [1] could not be

Table 4
Calculated conformer ratios.

	A	*B*	*C*	*D*	Relative conformer ratio
1	37,634	2366	–	–	16:1
2	31,878	8122	–	–	4:1
3	35,054	4946	–	–	7:1
4	2408	30,991	1147	5454	2:27:1:5
5	40,000	–	–	–	–
6	5733	34,267	–	–	1:6

Table 5
Dihedral angles of the conformers obtained from the MD simulations.

Substance	Region[a]	Φ	Ψ
1	A	−87.3°	172.9°
	B	63.8°	172.1°
2	A	−45.2°	−164.3°
	B	74.4°	−34.4°
3	A	−56.1°	173.7°
	B	43.8°	−164.6°
4	A	−51.1°	−0.6°
	B	−68.4°	164.1°
	C	66.1°	−37.9°
	D	58.0°	171.0°
5	A/B	−79.2°	173.4°
6	A	−62.1°	81.4°
	B	−65.5°	−105.1°

[a] The letters in this column correspond to the letters shown in the Φ/Ψ-plots.

affirmed by our calculations, whereas the experimental data (marked bold in Table 10) for both substances show, that only one conformer is existent in solution, which is consistent with the RDC values as well as the NOEs.

3. Conclusions

We successfully performed conformational analyses on six *N*-acetyl glucosamine derivatives. First, all signals in the ^{1}H NMR spectra were assigned employing different standard NMR methods. Afterwards, the configuration of the anomeric carbon atom of each carbohydrate was determined measuring the vicinal $^3J_{H_1,H_2}$ coupling constants and finally, it could be proven experimentally via the evaluation of RDCs and NOEs, that the calculated conformer ratios for the aromatic substances **1**–**5** are incorrect and only the favored conformers were verified. The additional conformers obtained from the MD simulations seem to be metastable and could not be observed on the experimental conditions we used. For substance **6** the RDCs could be measured successfully in two different alignment media, whereas a dramatic change in the conformer ratio depending upon the medium could not be affirmed. DMPC/DHPC bicells and $C_{12}E_5$/*n*-hexanol seem to align the favored

Table 6
Graphical representation of the calculated conformers.

	A	*B*	*C*	*D*
1	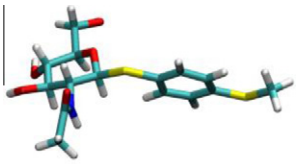	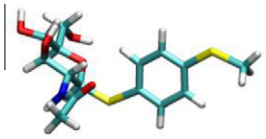		
2	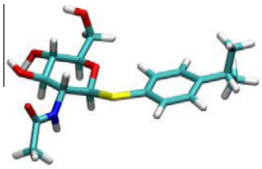	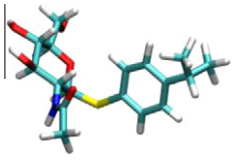		
3	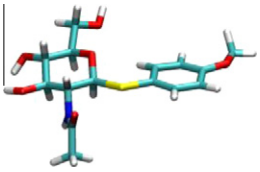	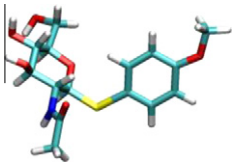		
4	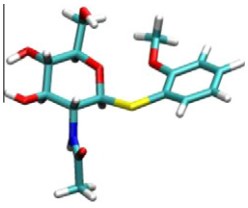	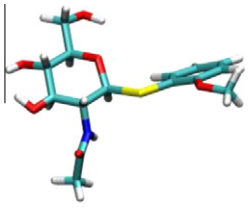	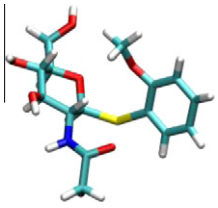	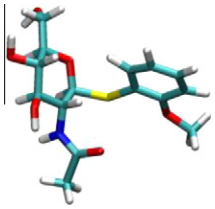
5	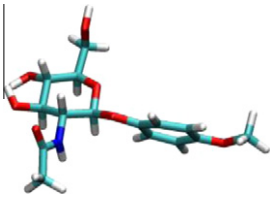			
6	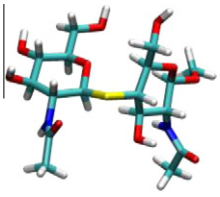	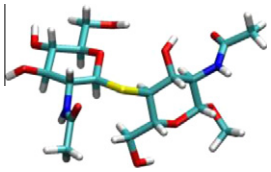		

Table 7
Results from REDCAT considering all calculated conformers.

Substance	Medium	Conformer ratio (A:B[:C:D])	Number of solutions[a]	RMSD	Q-Factor
1	Bicells	16:1	9219	0.17	0.1
		1:0	9172	0.09	0.05
		0:1	0	–	–
2	Bicells	4:1	8350	3.61	0.96
		1:0	8321	0.14	0.04
		0:1	1409	0.52	0.14
3	Bicells	7:1	2568	7.51	4.06
		1:0	8907	0.14	0.08
		0:1	0	–	–
4	Bicells	2:27:1:5	1806	1.95	0.26
		0:1:0:0	8864	0.27	0.04
		1:0:0:0	8426	0.37	0.05
		0:0:1:0	0	–	–
		0:0:0:1	0	–	–
5	Bicells	–	8771	0.07	0.04
6	Bicells	1:6	60	1.05	0.12
		1:16	1307	0.74	0.09
		0:1	6575	0.47	0.06
		1:0	0	–	–
	$C_{12}E_5$/*n*-hexanol	1:6	8481	0.33	0.06
		1:16	8875	0.22	0.04
		0:1	8944	0.21	0.04
		1:0	0	–	–

[a] Out of 10,000 error space samplings.

Table 8
Correlation plots for the ratios as calculated and the single favored conformer.

Substance	Medium	Correlation plots	
		Ratio as calculated	Favored conformer
1	Bicells	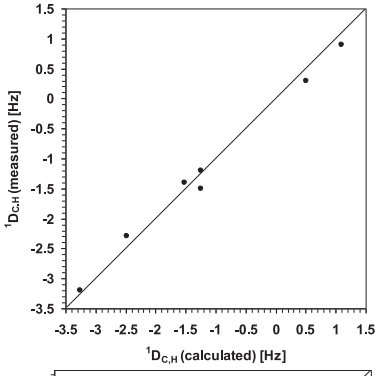	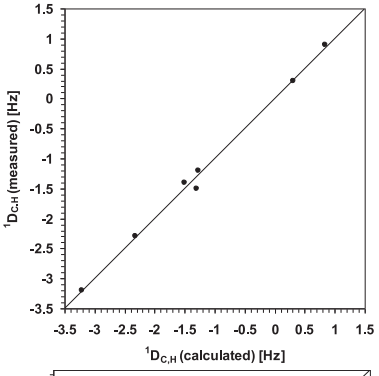
2	Bicells	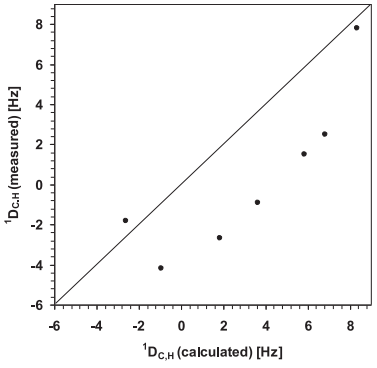	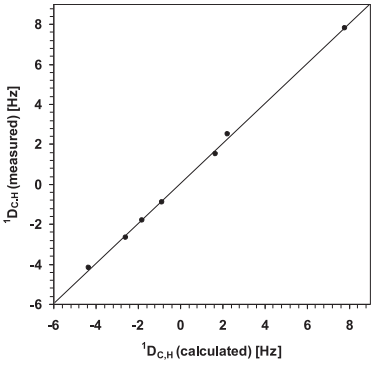

Table 8 (*continued*)

Substance	Medium	Correlation plots	
		Ratio as calculated	Favored conformer
3	Bicells	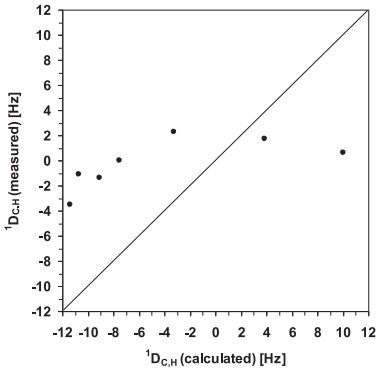	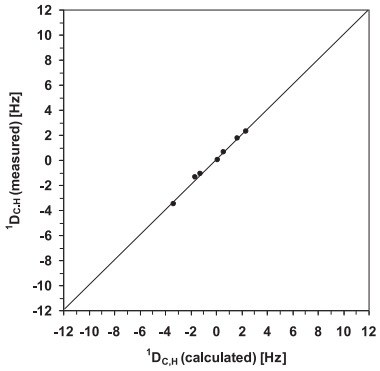
4	Bicells	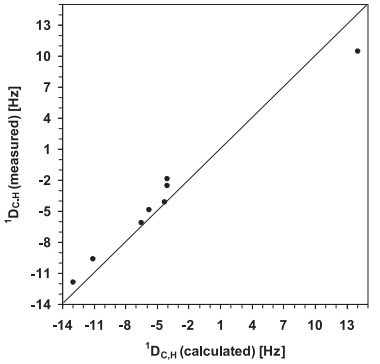	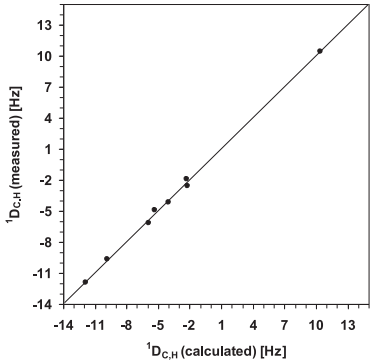
5	Bicells		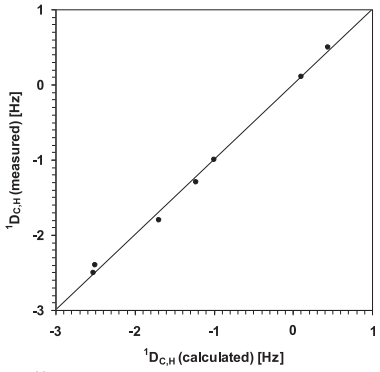
6	Bicells	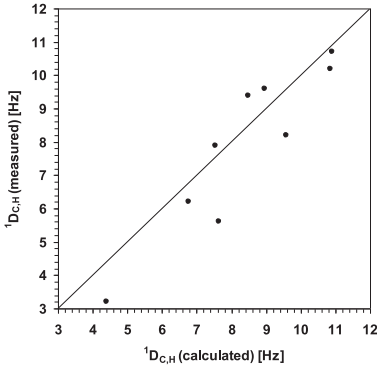	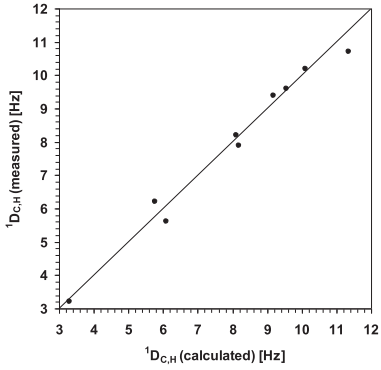

(*continued on next page*)

Table 8 (*continued*)

Substance	Medium	Correlation plots	
		Ratio as calculated	Favored conformer
	$C_{12}E_5$/*n*-hexanol	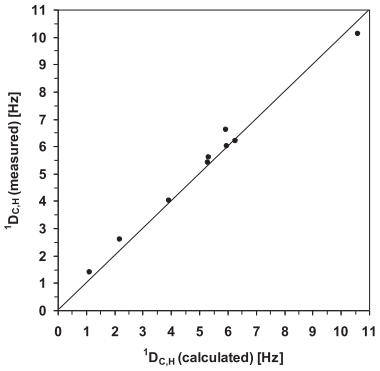	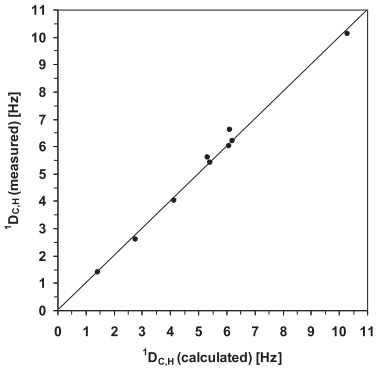

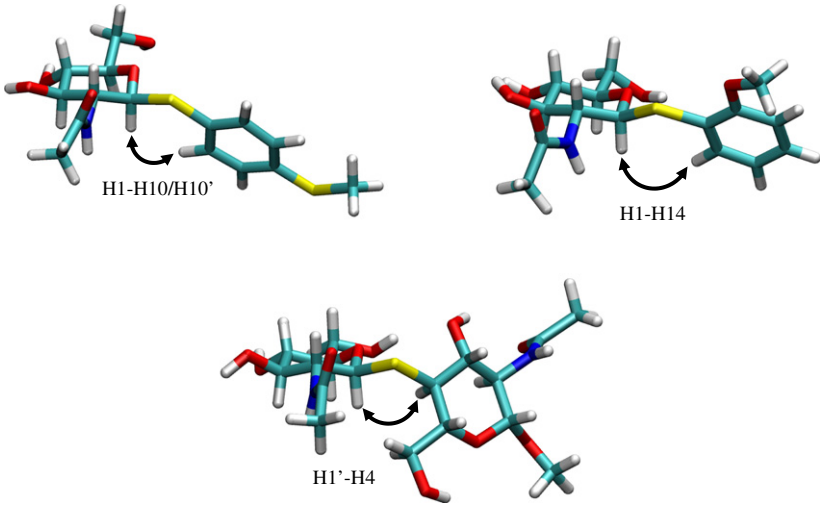

Fig. 5. NOEs made up by the favored conformer.

conformer **6**B more strongly. For the bicells the correlation between measured and calculated RDC values was best if only this favored conformer was considered. For $C_{12}E_5$/*n*-hexanol a small fraction of the conformer **6**A did not worsen the correlation for a conformer ratio of 1:16 compared to that for 0:1 (**6**A:**6**B). Because the measured NOEs for **6** requires the presence of **6**A of at least 1% a ratio of 1:16 is in better agreement with it.

Furthermore, several conformers as well as its populations reported by Fettke et al. [1] for **1**, **5** and **6** could not be validated theoretically and experimentally.

4. Experimental section

4.1. NMR spectroscopy

All NMR experiments were carried out using a Bruker Avance spectrometer operating at 500.17 MHz for ^{1}H using a Bruker BBFO probehead equipped with a *z*-gradient and a Bruker Variable Temperature Unit.

4.1.1. NOESY

The NOESY spectra were recorded using the *noesygpph* pulse sequence from the standard Bruker database. For the substances **1**–**5** a mixing time of 1 s and for substance **6** 0.8 s was used. In F_2 direction 2048 and in F_1 direction 512 data points were acquired with 128 scans per t_1 increment.

4.1.2. RDC measurement

For each substance measured in (DMPC/DHPC) bicelle medium two CLIP-HSQC experiments [16] at 38 °C and 20 °C respectively were arranged (see Supplementary material). These two different experiments were performed with the same NMR sample. For the isotropic case we additionally decided to use one without DMPC/DHPC. This led to better interpretable HSQC spectra, because the disturbing peaks of the alignment medium disappeared. The difference in the splitting of each signal at both temperatures corresponds to the $^1D_{C,H}$ value of the observed C–H pair.

For the $C_{12}E_5$/*n*-hexanol medium this was realized by performing one CLIP-HSQC experiment of substance **6** in the liquid crystalline medium and a second experiment of **6** in D_2O (each at 20 °C), whereas the difference in the signal splitting makes up again the $^1D_{C,H}$ value.

4.2. Sample preparation

For the standard NMR experiments all substances were solved in D_2O. To shift the HDO signal at 4.7 ppm upfield, some drops of DMSO were added to the solution of substance **1**. Otherwise, the H1 signal will overlap with the HDO signal. Because of the low solubility of the aromatic carbohydrates **1**–**5** we prepared a suspension of 5 mg carbohydrate in 1 ml D_2O, which was stirred for at least 10 min at room temperature. Afterwards, the precipitate

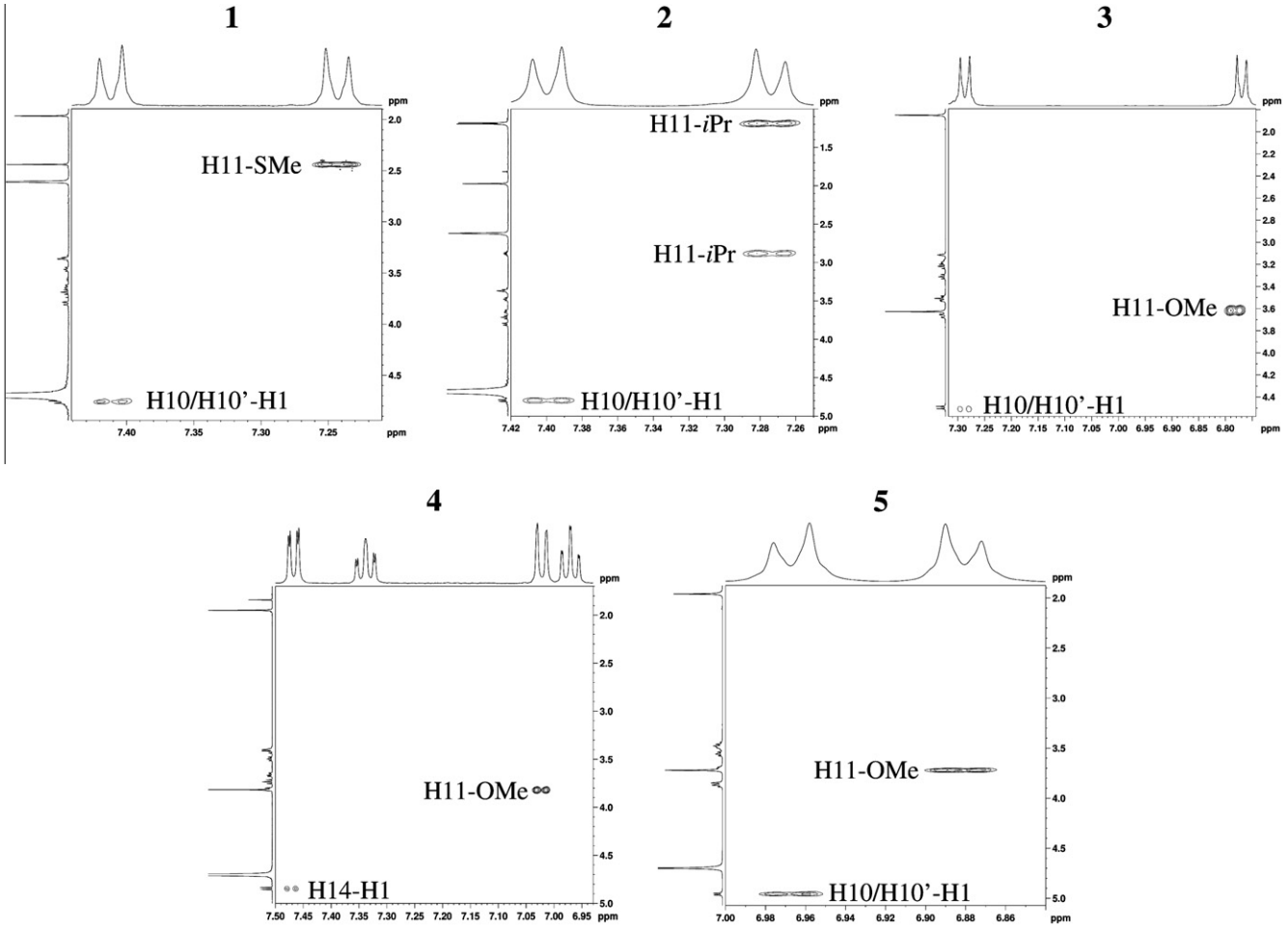

Fig. 6. Aromatic part of the NOESY spectra for the substances **1**–**5**.

was filtered off using a syringe filter which finally leads to a saturated solution of the carbohydrate.

The better solubility of substance **6** allowed the usage of higher concentrated samples of it. For this carbohydrate 10 mg of it were dissolved in 0.6 ml D_2O leading to a clear solution.

4.2.1. Bicelle system

A molar ratio of 3:1 (DMPC:DHPC) is necessary to achieve a bicelle diameter suitable for the measurement of RDC constants. A total lipid concentration of 10% was used resulting in a quadrupolar splitting of ~10–12 Hz (see Supplementary material) for the deuterium signal of D_2O. DHPC is hygroscopic and hydrolyses in the presence of water hence it should be handled in a glove box. For a typical NMR sample a 15% bicelle solution was prepared by weighing 10.9 mg of DHPC and 48.9 mg of DMPC in a glove box separately into a capped vial with septum. 0.2 ml of D_2O were added to each vial and the resulting mixtures were vortexed for several minutes resulting in a clear solution for DHPC and in a milky suspension for DHPC. The DHPC solution was then added to the content of the other vial and the product was vortexed. Afterwards this solution was frozen in liquid nitrogen, warmed up to room temperature and vortexed again for at least 1 min. This procedure was repeated until the resulting liquid was clear. To this liquid 0.2 ml of a solution of the carbohydrate (prepared as explained before) were added and the aforesaid process was repeated again leading to 0.6 ml of a bicelle/carbohydrate solution with the above mentioned total lipid concentration of 10%. This solution was then transferred to an NMR sample tube.

4.2.2. $C_{12}E_5$/n-hexanol system

For $r = 0.87$ [13] 25 μl $C_{12}E_5$ and 0.5 ml D_2O were mixed and vortexed well. Afterwards, 9 μl of *n*-hexanol were added in three steps per 3 μl, while vortexing thoroughly between the steps. The final liquid crystalline product should be a bluish gleaming viscous fluid containing small bubbles. For this sample a quadrupolar splitting of ~30 Hz (see Supplementary material) was measured for the ^2H signal of D_2O. To this medium 5 mg carbohydrate were added and solved by warming up the sample tube to 35 °C.

4.3. Calculations

Molecular dynamics (MD) simulations were performed with the TINKER software package [18] (available from http://dasher.wustl.edu/tinker/) and the GLYCAM06 force field [24,25]. Because this force field was not parametrized for TINKER we changed the standard GLYCAM parameter file to meet the TINKER parameter file format. Furthermore, we introduced additionally needed parameters from [1].

The MD simulations were performed at 300 K in an NVT ensemble. Bulk water was simulated using the periodic boundary condition (PBC) by placing the energy optimized molecule in a $20 \times 20 \times 20$ Å box together with 300 water molecules. During the first simulation steps this box was allowed to expand until the resulting density of the system reaches a value of about 1 g/cm^3. A total of 20 ns was simulated with a time step length of 1.0 fs and the time between dumps was 0.5 fs yielding 40,000 dumps. The results of this simulation have been visualized by

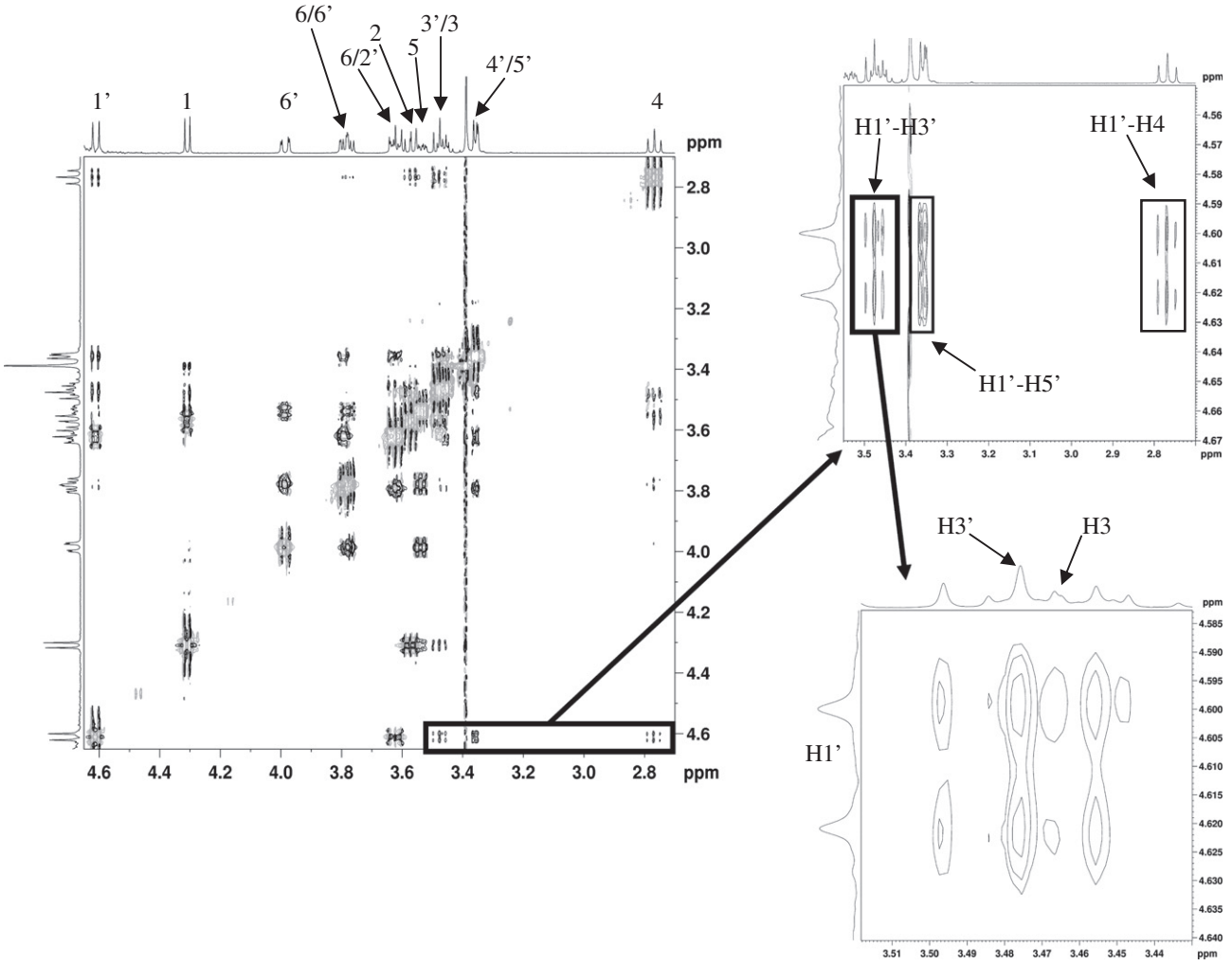

Fig. 7. NOESY spectrum for substance **6** including important zoomed parts.

Table 9
Calculated dihedral angles for **6** compared to that from [1].

Torsional angle	Conformer	Our values	Conformer in [1]	Values from [1]
Φ	**A**	**54.6**°	D	61°
Ψ		**−167.5**°		−159° (201°)
Φ	**B**	**51.7**°	C	49°
Ψ		**4.3**°		4°

Table 10
Calculated dihedral angles for **1** and **5** compared to that from [1].

Substance	Conformer	Torsional angle	Values	Substance in [1]	Conformer in [1]	Torsional angle	Values from [1]
1	**A**	Φ	**35.4**°	**3**	F	Φ	57°
		Ψ	**172.9**°			Ψ	177°
	B	Φ	172.9°		E	Φ	179°
		Ψ	172.1°			Ψ	170°
5	–	Φ	**45.2**°	**5**	E	Φ	44°
		Ψ	**173.5**°			Ψ	184°

VMD [19] (http://www.ks.uiuc.edu/Research/vmd/). The same program was used to perform an RMSD overlay for all possible conformations of the corresponding substance.

To determine the theoretical RDC constants from the modelled structures we used the REDCAT program [22] (freely downloadable from http://ifestos.cse.sc.edu/software.php).

Acknowledgments

We thank Prof. M.G. Peter and Dr. Dirk Peikow for the syntheses of the investigated carbohydrates and the Deutsche Forschungsgemeinschaft (DFG) for supporting this work (KL 754/8).

Appendix A. Supplementary material

Supplementary data associated with this article can be found, in the online version, at doi:10.1016/j.jmr.2011.06.029.

References

[1] A. Fettke, D. Peikow, M.G. Peter, E. Kleinpeter, Tetrahedron 65 (2009) 4356–4366.
[2] D. Peikow, Synthese und Glycosidasehemmung von Thio-analogen Kohlenhydraten PhD-thesis, University of Potsdam, 2006. <http://opus.kobv.de/ubp/volltexte/2006/1119/>.
[3] F. Tiang, H.M. Al-Hashimi, J.L. Craighead, J.H. Prestegard, J. Am. Chem. Soc. 123 (2001) 485–492.
[4] A. Silipo, Z. Zhang, F.J. Cañada, A. Molinaro, R.J. Linhardt, J. Jiménez-Barbero, ChemBioChem. 9 (2008) 240–252.
[5] M. Martin-Pastor, C.A. Bush, Biochemistry 39 (2000) 4674–4683.
[6] M. Martin-Pastor, C.A. Bush, J. Biomol. NMR 19 (2001) 125–139.

[7] G.R. Kiddle, S.W. Homans, FEBS Lett. 436 (1998) 128–130.
[8] C.M. Thiele, V. Schmidts, B. Böttcher, I. Louzao, R. Berger, A. Maliniak, B. Stevenson, Angew. Chem. Int. Ed. 48 (2009) 6708–6712.
[9] H. Shimizu, A. Donohue-Rolfe, S.W. Homans, J. Am. Chem. Soc. 121 (1999) 5815–5816.
[10] J.A. Losonczi, M. Andrec, M.W.F. Fischer, J.H. Prestegard, J. Magn. Reson. 138 (1999) 334–342.
[11] G. Kummerlöwe, B. Luy, Annu. Rep. NMR Spectrosc. 68 (2009) 193–230.
[12] P.J. Bolon, J.H. Prestegard, J. Am. Chem. Soc. 120 (1998) 9366–9367.
[13] M. Rückert, G. Otting, J. Am. Chem. Soc. 122 (2000) 7793–7797.
[14] A. Germer, M.G. Peter, E. Kleinpeter, J. Org. Chem. 67 (2002) 6328.
[15] A. Germer, C. Mügge, M.G. Peter, A. Rottmann, E. Kleinpeter, Chem. Eur. J. 9 (2003) 1964.
[16] A. Enthart, J.C. Freudenberger, J. Furrer, H. Kessler, B. Luy, J. Magn. Reson. 192 (2008) 314–322.
[17] G. Kummerlöwe, S. Schmitt, B. Luy, Open Spectrosc. J. 4 (2010) 16–27.
[18] J.W. Ponder, TINKER, Software Tools for Molecular Design, Washington University School of Medicine, Saint Louis, 2004.
[19] W. Humphrey, A. Dalke, K. Schulten, J. Mol. Graphics 14 (1996) 33–38.
[20] H. Sun, E.J. d'Auvergne, U.M. Reinscheid, L.C. Dias, C.K.Z. Andrade, R.O. Rocha, C. Griesinger, Chem. Eur. J. 17 (2011) 1811–1817.
[21] J.H. Prestegard, X. Yi, Structure and Dynamics of Carbohydrates using Residual Dipolar Couplings, in: J.F.G. Vliegenthart, R.J. Woods (Eds.), NMR Spectroscopy and Computer Modeling of Carbohydrates, ACS Symposium Series 930, American Chemical Society and Oxford University Press, 2006, 40–59.
[22] H. Valafar, J.H. Prestegard, J. Magn. Reson. 167 (2004) 228–241.
[23] http://tesla.ccrc.uga.edu/software/REDCAT/manual/tut4Dyn2AVG.html.
[24] R. Woods, R. Dwek, C. Edge, B. Fraser-Reid, J. Phys. Chem. 99 (1995) 3832.
[25] Glycam06 parameters. <http://glycam.ccrc.uga.edu/ccrc/pages/temp/gl_params.jsp>.